Title: Comparative genomics of *Pseudomonas syringae* pathovar *tomato* reveals novel chemotaxis pathways associated with motility and plant pathogenicity

Authors: Christopher R. Clarke[1], Byron W. Hayes[1], Brendan J. Runde[1], Eric Markel[2], Bryan M. Swingle[2,3], and Boris A. Vinatzer[1]

Affiliations: [1]Department of Plant Pathology, Physiology, and Weed Science. Virginia Tech. Blacksburg, VA, USA.

[2] Emerging Pests and Pathogens Research Unit, Robert W. Holley Center for Agriculture and Health, United States Department of Agriculture-Agricultural Research Service, Ithaca, NY, USA.

[3]Plant Pathology and Plant-Microbe Biology Section, School of Integrative Plant Science, Cornell University, Ithaca, NY, U.S.A.

Corresponding author: Christopher Clarke, thechrisclarke@gmail.com

Abstract

The majority of bacterial foliar plant pathogens must invade the apoplast of host plants through points of ingress, such as stomata or wounds, to replicate to high population density and cause disease. How pathogens navigate plant surfaces to locate invasion sites remains poorly understood. Many bacteria use chemical-directed regulation of flagellar rotation, a process known as chemotaxis, to move towards favorable environmental conditions. Chemotactic sensing of the plant surface is a potential mechanism through which foliar plant pathogens home in on wounds or stomata, but chemotactic systems in foliar plant pathogens are not well characterized. Comparative genomics of the plant pathogen *Pseudomonas syringae* pathovar *tomato* (Pto) implicated annotated chemotaxis genes in the recent adaptations of one Pto lineage. We therefore characterized the chemosensory system of Pto. The Pto genome contains two primary chemotaxis gene clusters, *che1* and *che2*. The *che2* cluster is flanked by flagellar biosynthesis genes and similar to the canonical chemotaxis gene clusters of other bacteria based on sequence and synteny. Disruption of the primary phosphorelay kinase gene of the *che2* cluster, *cheA2*, eliminated all swimming and surface motility at 21^{o}C but not 28^{o}C for Pto. The *che1* cluster is located next to Type IV pili biosynthesis genes but disruption of *cheA1* has no observable effect on twitching motility for Pto. Disruption of *cheA2* also alters *in planta* fitness of the pathogen with strains lacking functional *cheA2* being less fit in host plants but more fit in a non-host interaction.

Introduction

Pseudomonas syringae pv. *tomato* (Pto) is a common bacterial pathogen adapted to live in both agricultural and non-agricultural environments. Pto is most intensively studied for its role in causing bacterial speck disease in tomato. The Pto population is comprised of multiple closely related lineages of the pathogen. The PtoT1 lineage (which includes the well-studied eponymous member PtoT1 (Almeida et al. 2009) has dominated the population for the last 60 years in North America and Europe (Cai et al. 2011). In prior decades, the PtoJL1065 and PtoDC3000 lineages were likely the dominant field populations (Cai et al. 2011). PtoDC3000 is actually more closely related to pathogens of *Brassicaceae* than to PtoJL1065 and PtoT1 and its host range includes members of the *Brassicaceae* family (Yan et al. 2008). Strains in the PtoT1 lineage are specialists in tomato (Cai et al. 2011) but can also infect other *Solanaceae* (Clarke et al. 2014).

To identify the genetic features that might contribute to the recent emergence of the PtoT1 lineage, we previously sequenced and analyzed the genomes of several closely related Pto strains (Cai et al. 2011). One of the most striking non-plant-defense-related features in the genomes of PtoT1-lineage strains was the presence of several non-synonymous single nucleotide polymorphisms (SNPs) in Methyl-accepting Chemotaxis Proteins (MCPs) in Pto. We therefore hypothesized that the fine tuning of chemotaxis pathways is involved in the adaptation of Pto to its tomato host. We thus sought to identify the genetic basis for chemotaxis in Pto and characterize the importance of chemotaxis for Pto motility and interaction with plant hosts.

Many bacteria use chemotaxis pathways to control flagella-driven motility in response to environmental stimuli in a "biased random walk" (Berg & Brown 1972). Bacteria fluctuate between moving forward (running) and reorienting (tumbling) in a controlled manner, where running is favored in the presence of increasing levels of favorable chemical cues and tumbling is favored in the presence of unfavorable chemical cues. Specific chemical cues are recognized in the periplasm by the ligand-binding domains of membrane-spanning MCPs, and signals are propagated, through a highly conserved cytoplasmic HAMP domain (Aravind & Ponting 1999), to a histidine-aspartate phosphorelay system (see (Parkinson et al. 2015; Wadhams & Armitage 2004) for review). The final output is the regulation of flagellar motor rotation resulting in movement towards attractants and away from repellents. The genes involved in the two-component phosphorelay, *cheA* and *cheY*, are essential for chemotaxis in *Escherichia coli* (Parkinson & Houts 1982), *P. aeruginosa* (Ferrández et al. 2002), and other bacteria (Porter et al. 2011).

Chemotaxis is also linked to type IV (T4) pili-dependent motility, such as twitching motility (Kirby 2009), in some bacteria. For example, *P. aeruginosa* has one chemotaxis pathway for controlling flagellar motility and a second *che* gene cluster involved in T4 pili formation, motility (Darzins 1994; Whitchurch et al. 2004), and biofilm formation (Hickman et al. 2005). Interestingly, T4 pili have previously been implicated as important in epiphytic colonization of plants (Roine et al. 1998) and have been demonstrated to be essential for virulence and surface motility by a *P. syringae* pv. *tabaci* strain (Nguyen et al. 2012; Taguchi & Ichinose 2011). Also significant work has been done on the role of T4 pili in the insect-vectored plant pathogen *Xyella*

fastidiosa (see (De La Fuente et al. 2008; Li et al. 2007)for examples) and the plant pathogen *Acidovorax avenae* (Bahar et al. 2009).

For plant-associated microbes, chemotaxis pathways have been best studied in diazotrophs. The α-proteobacterium *Sinorhizobium meliloti*, has a chemotaxis system significantly divergent from that of *E. coli* (Schmitt 2002) with two *cheY* genes but only one *cheA* (Scharf et al. 2016). CheY2 acts as the master switch for the flagellar motor like *E. coli* CheY (Sourjik & Schmitt 1996), and CheY1 compensates for the lack of CheZ by acting as a phosphate sink since it can dephosphorylate CheY2 through CheA (Riepl et al. 2008). The phosphate sink regulatory mechanism of the secondary CheY proteins is also found in the α-proteobacterium *Rhodobacter sphaeroides* (Shah et al. 2000). In *Rhizobium leguminosarum*, both chemotaxis clusters contribute to motility but only one is responsible for chemotactic responses to host chemical cues in the rhizosphere (Miller et al. 2007). Also in *Azospirillum brasilense* motility, and specifically chemotaxis, is necessary for successful colonization of its host's roots (Van de Broek et al. 1998). The soil-borne close relative of *P. syringae, Pseudomonas fluorescens,* is also chemotactic and is attracted to several amino acid exudates of tomato roots (Oku et al. 2012).

Chemotaxis pathways are also required for optimal colonization of roots by soil-borne plant pathogens. The plant pathogens *Agrobacterium tumefaciens* (Hawes & Smith 1989), *Ralstonia solanacearum* (Yao & Allen 2006), and *Phytophthora sojae* (Morris & Ward 1992), all rely on functional chemotaxis to effectively home in on host roots. However, chemotaxis has never been directly shown as required for plant pathogenicity after locating host roots.

In contrast to soil-borne pathogens, chemotaxis has been directly implicated in plant colonization by the foliar pathogens *Xanthomonas campestris* (Kamoun & Kado 1990) and *Xanthomonas citri* (Moreira et al. 2015). There have been several recent advances implicating chemoperception in the interaction of *P. syringae* with plant hosts. Chemotaxis-associated genes were shown to be up-regulated during the epiphytic phase of invasion of the bean pathogen *Pseudomonas syringae* pv. *syringae* (Yu et al. 2013) and to play a role in vascular pathogenicity of the olive pathogen *Pseudomonas syringae* pv. *savastanoi* (Matas et al. 2012). Moreover, it has been shown that Pto swims towards open stomata of *Arabidopsis thaliana* leaves (Melotto et al. 2006) suggesting that *P. syringae* can sense some chemical cues released from stomata.

To determine the extent to which Pto employs chemotaxis and to determine its genetic basis, we characterized the chemotactic systems of Pto and elucidated the importance of chemosensory systems in regulation of bacterial motility and plant pathogenicity.

Materials and Methods

cheY phylogenetic analysis

cheY gene sequences of bacteria with previously characterized chemotaxis pathways and select additional *P. syringae* strains were obtained from Genbank and aligned using Megalign (DNA*, Madison, WI, USA). A neighbor joining tree was built based on this alignment using 1000 trials and a random seed of 111. The species(strains) of bacteria included were *P. syringae* (PtoDC3000 (Buell et al. 2003), PtoT1 (Almeida et al. 2009), Pph1448a (Joardar et al. 2005), Psy642 (Clarke et al. 2010)), *P. aeruginosa* (PAO1 (Stover et al. 2000)), *S. enterica*

(typhimurium (Stock et al. 1985)), *E. coli* (K-12 (Blattner et al. 1997)), *Rhodobacter sphaeroides* (241 (Ward et al. 1995)), *S. meliloti* (RU11001), *Bacillus subtilis* (168 (Kunst et al. 1997)).

Plant and bacterial growth

Solanum lycopersicum cv. Heinz or cv. Rio Grande (tomato) seeds were sowed into 1:1 mix of promix BX (Premier Horticulture, Quebec, Candada) and metromix (Sungro, Sebe Beach, Canada) soil. *A. thaliana* ecotype Columbia seeds were stratified for 3 days in water at 4^{o}C and then sowed into Sunshine #1 (Sungro, Sebe Beach, Canada) soil. All plants were grown for 4-5 weeks under a laboratory growth light shelf at 22^{o}C and 12-hour light cycles.

All bacteria were grown overnight at 28^{o}C on King's B (KB, (King et al.)) plates with 1.5% agar and 25µg/ml tetracycline (all strains included the empty vector pme6010 to use tetracycline as an antibiotic marker) before use in assays. For measuring growth of strains in liquid culture, bacteria were diluted in 10mM $MgSO_4$ to an optical density at 600nm wavelength (OD_{600}) of 0.01. 5µL was added to 5ml a test tube of either liquid KB media or liquid Minimal Media (MM) (Huynh 1989) and placed in a 28^{o}C shaking incubator. 10µL of the media was removed from the tubes at the indicated time points, diluted, and then plated on KB-tetracycline plates. Plates were incubated at 28^{o}C, the number of colony forming units were counted, and the number of CFUs/ml in the test tube at the sample time was calculated.

Swim and swarm plates

Swim and swarm plates were made by making standard KB media plates with the indicated agar concentrations instead of the standard 1.5% agar concentration and adding tetracycline to 25µg/ml. Swim and swarm plates were always used 4-5 hours after they were made. 2µL of bacteria diluted in 10mM $MgSO_4$ to an OD600 of 0.01 were pipetted onto the plates, with 3 bacteria strains/plate. Strains being directly compared were inoculated onto the same set of plates to account for plate-to-plate variability. 10 minutes after the inoculation, the lid of the plate was lightly sprayed with water and the plate was flipped upside down into the lid (so that the wet inside of the lid is at the bottom, followed by an air gap, followed by the bacteria on the agar media at the top) and sealed with parafilm. Maximum cross section of the colony spread was measured after a two-day incubation at 28^{o}C or 21^{o}C. In these plates, if a strain is either non-motile or unable to tumble to change directions the bacteria cannot spread beyond the point of inoculation. Fully motile and chemotactic bacteria spread on the plate due to local depletion of nutrients leading to a nutrient gradient and chemotactically driven swimming motility toward local regions with more nutrients.

Split capillary assay

Capillary assays were modified from (Adler 1973). A ring of grease was created on a glass coverslip. Bacteria diluted in 10mM $MgSO_4$ to an OD600 of 0.01 were pipetted into the grease ring to form a pool of the bacteria. One 1µL capillary tube (Drummond Scientific, Broomall, PA) was filled with 10mM $MgSO_4$, sealed at one end with parafilm, and inserted at the open end into the pool of bacteria. A second capillary tube was filled with KB media, sealed at one end with parafilm, and inserted at the open end into the pool of bacteria. Extra grease was placed on

top of the capillary tubes where they contact the grease ring and the pool was sealed with a coverslip on the top (see **Figure S6**). The coverslip sandwich was left undisturbed for 45 minutes. Following the 45-minute incubation the contents of the capillary tube were diluted, plated onto solid KB-tetracycline plates, and incubated at 28^{o}C for two days The number of colony forming units (CFUs) originating from each capillary tube was counted and used to calculate the ratio of the number of CFUs from the KB-containing capillary over the number of CFUs from the matching 10mM $MgSO_4$ capillary.

Creation of chemotaxis disruption and deletion mutants and molecular cloning of chemotaxis genes

Genome disruptions of the *cheA1* and *cheA2* genes were created via the *P. syringae* gene disruption construct pBAV208 using a previously described approach (Clarke et al. 2010) and the primers listed in **Table S2**. The disruptions result in strains with two fragments of the *cheA* genes. The *cheA1* disruption mutants have a 5' *cheA1* fragment with an in-frame stop codon at position 261 and a 3' fragment starting with a stop codon. The *cheA2* disruption mutants have a 5' *cheA2* fragment with an in-frame stop codon at position 281 and a 3' fragment starting with a stop codon. Plasmids were conjugated into PtoDC3000 and Pto1108 via triparental mating. Major results were confirmed with second, independent disruption mutants of *cheA1* and *cheA2* in both PtoDC3000 and Pto1108. Disruption mutants are designated as either *cheA1*$^{-}$ *cheA2*$^{-}$ strains throughout this paper.

The PtoDC3000 Δ*cheA1*, Δ*cheA2* and Δ*cheA1cheA2* deletion mutant strains were constructed using the recombineering methods described in (Swingle et al. 2010) and (Bao et al. 2012). The Δ*cheA1* mutant was constructed by transforming PtoDC3000 containing pUCP24/recTE with a recombineering substrate designed to replace the *cheA1* gene with the kanamycin resistance encoding *neo* gene flanked by modified *frt* sequences (*frt-neo-frt*). The *cheA1* deletion recombineering substrate was amplified by PCR using primers oSWC06647 and oSWC06648 and pKD4 as a template. This product contained the *frt-neo-frt* cassette flanked by 80 bp sequences homologous to PtoDC3000 genome coordinates 996501-996580 and 994354-994433 at the left and right end, respectively. Kanamycin resistant recombinants were selected and confirmed to contain the *frt-neo-frt* cassette in the correct location by PCR. The *cheA1* deletion recombinants were then transformed with pCPP5264, which expresses the FLP recombinase and catalyzes site-specific recombination between *frt* sequences to remove the *neo* gene. The *neo* gene was confirmed to be deleted by PCR and the recombinant strains were confirmed to have lost the pUCP24/recTE and pCPP5264 plasmids. The structure of the mutant was confirmed by sequence analysis to consist of the first 6 codons of the *cheA1* gene, fused in frame to the 28 codon *frt* scar and followed by 6 terminal codons of the *cheA1* gene.

The *cheA2* deletion strains were then constructed using recombineering to introduce the mutation into wild-type and Δ*cheA1* backgrounds to yield the *cheA2* and *cheA1cheA2* deletion strains. The *cheA2* recombineering substrate was generated using long flank homology PCR as described in (Swingle et al. 2010). The *cheA2* recombineering substrate was composed of the *frt-neo-frt* cassette with a 516 bp right flank and 556 bp left flank homologous to PtoDC3000 genome coordinates 2166604-2167120 and 2169335-2169890. The *cheA2* deletion recombineering

substrate was used to transform wild-type and *cheA1* strains containing the pUCP24/recTE recombineering plasmid; recombinants were selected for resistance to kanamycin. The integration of the *frt-neo-frt* deletion cassette at the correct location was confirmed by PCR. These strains were then transformed with pCPP5264 to catalyze the excision of the *neo* gene. PCR was used to demonstrate that the *neo* gene had been deleted and the pUCP24/recTE pCPP5264 plasmid was cured from the *cheA2* deletion strains. The final structure of the deletion mutants was confirmed by sequencing to consist of the first 6 codons of the *cheA2* gene fused in frame to the *frt* scar and the terminal six codons of *cheA2*.

For the complementation strains, *cheA1* and *cheA2* were individually cloned into the *P. syringae* expression vector pme6010 using a previously described approach (Clarke et al. 2013) under control of the constitutive *npt2* promotor and the primers listed in **Table S2**. *cheA1* was cloned including 25bp upstream of the start codon and *cheA2* was cloned including 14bp upstream of the start codon. The pme6010 plasmids containing *cheA1* and *cheA2* were conjugated into PtoDC3000 and Pto1108 wild type and *cheA1*/*cheA2* disruption/deletion strains via triparental mating.

Plant infection and hypersensitive response assays

Comment [JHC1]:

Plant infections were carried out under a laboratory growth shelf (12 hour light cycle) as previously described (Clarke et al. 2013). Briefly, spray infections were performed with 0.01 OD_{600} of freshly grown bacteria on 4- or 5-week-old tomato or *A. thaliana* plants 24 hours after the plants were sprayed with water and placed under a humidity dome. High humidity was maintained for 16 hours following infection and leaves were sampled 4 days post infection using a 4mm cork borer for quantifying total bacterial growth (both endophytic and epiphytic populations) as previously described (Clarke et al. 2013) using KB-tetracycline plates. For hypersensitive response assays, 4- or 5-week-old Arabidopsis plants were infiltrated with 0.3 OD_{600} bacteria on one half of the leaf. The presence of leaf collapse of the infiltrated part each leaf, indicating a hypersensitive response, was checked for after 18 hours or 40 hours for the PtoDC3000 and Pto1108 strains, respectively.

Comment [JHC2]:

Results

Single nucleotide polymorphisms in a recently emerged Pto lineage are enriched in chemotaxis-associated genes.

The genome sequences of the extremely closely related strains within the T1 lineage of Pto were previously compared to identify single nucleotide polymorphisms (SNPs) as candidates for the recent success of the PtoT1 lineage in tomato field populations in the past 50 years (Cai et al. 2011). Only 265 SNPs are present among the genomes of these strains (Cai et al. 2011). Seven non-synonymous SNPs were in the coding sequence of putative MCPs. This enrichment of SNPs in MCPs, suggests that chemo-detection systems are involved in the adaptation of the Pto lineage on tomato. Six of the seven non-synonymous SNPs are in the periplasmic domain of the MCPs (**Figure S1**), which is the domain responsible for recognizing specific chemoattractants/repellants (Parkinson et al. 2015). This pattern suggests that adaption in recognition of chemical compounds in the Pto lineage is potentially contributing to the recent

clonal expansion of the PtoT1 lineage. We therefore proceeded to characterize the chemosensory system of Pto in both the model strain PtoDC3000 and a genetically-tractable representative of the PtoT1 lineage in which the SNPs were identified, strain PtoNCPPB1108 (Pto1108 for short, **Table 1**).

The Pto genome contains two primary chemotaxis gene clusters

The previously sequenced Pto genomes (Buell et al. 2003; Cai et al. 2011) all have two gene clusters with canonical *cheA-cheY* two-component phosphorelays and three other clusters of putative chemotaxis-associated genes but lacking the histidine kinase *cheA* and response regulator *cheY* genes (**Figure 1A, Table S1).** The *che1* cluster is neighbored by genes associated with pili biosynthesis and syntenically similar to the *che2* cluster in *P. aeruginosa* (Kato et al. 2008). The *che2* cluster is syntenically similar to the *che* clusters of *E. coli* and *P. aeruginosa* (Kato et al. 2008) and immediately downstream of flagellar-biosynthesis genes like in the genomes of many other gram-negative bacteria.

Phylogenetic analysis of *cheY* gene sequences revealed that Pto *cheY2* clusters with high support (bootstrap = 100) with *cheY* genes known to be essential for flagellar regulation in other gammaproteobacteria (**Figure 1B**). Pto *cheY1* clusters with *cheY* genes not associated with flagellar motility in other bacteria. We therefore hypothesized that the Pto *che2* pathway is the canonical chemotaxis pathway regulating flagellar switching and the *che1* pathway has a distinct role, potentially functioning in regulation of pili-based motility.

The Pto genome encodes three additional non-canonical chemotaxis gene clusters. Like *che2,* the *che3* cluster is also flanked by flagellar biosynthesis genes. The *che4* and *che5* clusters each contain a putative non-canonical histidine kinase–response regulator two-component system, as well as *cheB* and *cheR*, which encode receptor-modifying enzymes, and *cheW*, which codes for an adaptor protein (**Figure 1A**). The Pto genome encodes 48 annotated MCPs in total.

The *che2* pathway in Pto regulates swimming motility

To assess the importance of the two major chemotaxis gene clusters, we created disruptions in the main signal transduction genes of the *che1* and *che2* clusters, *cheA1* and *cheA2,* individually in PtoDC3000 and Pto1108. The disruption mutants are referenced as *cheA1*$^-$ and *cheA2*$^-$ throughout the manuscript and figures. We also created in-frame gene deletions of *cheA1* and *cheA2* in PtoDC3000. The deletion mutants are referenced as Δ*cheA1* and Δ*cheA2*. We quantified swimming motility using low-agar-concentration (0.28%) KB swim plates that quantify flagellar-based motility and chemotactic function (see methods). *cheA2* was essential for motility of both PtoDC3000 and Pto1108 in the swim plates (**Figure 2A, Figure S2A**) and phenotypically identical to the *fliC* deletion mutant of PtoDC3000. The same phenotypes were observed with second, independent disruption mutants of *cheA1* and *cheA2* in both the PtoDC3000 and Pto1108 background. Complementation of *cheA2* in the PtoDC300*cheA2*$^-$ background restored swimming motility, but not to the level of the wild type strain (**Figure 2A**), potentially because the disruption insert was polar leading to misregulation of other genes in the *che2* cluster or non-optimized expression of *cheA2* (See **Figure 1A** and **Table S1**).

Deleted: and in-frame gene deletions of *cheA1* and *cheA2* in PtoDC3000.

To determine whether *cheA2* is essential for motility or only chemotactic regulation of motility, the swimming behavior of the strains were observed in liquid KB media using dark-field microscopy at 400x magnification. Both Pto1108*cheA2*$^-$ and PtoDC3000 *cheA2*$^-$ exhibited a "smooth-swimming" phenotype – motile, but unable to tumble to change swimming direction. Pto1108*cheA1*- and PtoDC3000 *cheA2*$^-$ both swam and tumbled similar to wild type strains(**Videos 1-3**). Flagellar mutants, in contrast to the *cheA2* mutants, are completely non-motile in this assay.

Additionally, in a variant of the classic capillary assay (Adler 1973) which tests chemotactic function based on the ability of bacterial cells to preferentially move into a nutrient-rich medium, *cheA2* was necessary for full chemotactic function in PtoDC3000 (**Figure 2B**). The *cheA2*$^-$ dependent aberrations in these assays are indicative of loss of directional control of swimming motility and not general defects in growth, because the PtoDC3000 and Pto1108 wild type and chemotaxis disruption mutant strains replicate at equivalent rates in both liquid plant-apoplast-mimicking Minimal Media (MM) and rich KB media (**Figure 3, Figure S3A**).

Swim plate motility was also eliminated in the PtoDC3000 Δ*cheA2* deletion mutant and mostly rescued by ectopic expression of *cheA2* (**Figure S2B**). The PtoDC3000 Δ*cheA1* deletion mutant was also partially impaired in swimming motility on swim plates, but complementation of *cheA1* did not rescue the swimming defect (**Figure S2B**). *Pto*DC3000 Δ*cheA1* grew slower than wild type in liquid culture (**Figure S3B**) suggesting a general growth defect in this strain, potentially due to changes in the duplication state of an unstable region in the PtoDC3000 genome (Bao et al. 2014). We therefore conclude that mutations in *cheA2* but not *cheA1* compromise regulation of the flagellar motor in both PtoDC3000 and Pto1108, demonstrating that the *che2* cluster is the primary cluster responsible for controlling flagellar-mediated chemotaxis. Because of the observed growth defect in the chemotaxis deletion mutants, we primarily relied on the disruption mutants in the subsequent assays.

Type 4 (T4) pili-regulated twitching motility is not controlled by the *che1* pathway in Pto

Because the *che1* gene cluster is flanked by a gene cluster annotated to encode for components of T4 pili, we hypothesized that the *che1* cluster might play a role in chemotactic control of T4 pili similar to the *che2* cluster of *P. aeruginosa* (Whitchurch et al. 2004). To test this hypothesis, we employed KB plates with different agar concentrations (0.4 – 1.3%) that allow for the observation of surface motility. We quantified surface motility by inoculating these plates with wild type PtoDC3000 and the PtoDC3000 *cheA2*$^-$ and PtoDC3000 *cheA1*$^-$ disruption mutants. We also inoculated the surface motility plates with PtoDC3000 Δ*fliC* (Clarke et al. 2013) and PtoDC3000 Δ*pilA* (a T4 pili-deficient deletion mutant, (Roine et al. 1998)) as controls for strains deficient in surface swarming and twitching motility respectively. PtoDC3000 Δ*pilA* is mostly non-motile on these plates (**Figure 4A)**, similar to previous observations (Roine et al. 1998), though would occasionally expand slightly beyond the inoculation site. PtoDC3000 Δ*fliC* and PtoDC3000 *cheA2*$^-$ were both motile starting at 0.6% agar concentration (**Figure 4A-B**). PtoDC3000 *cheA1*$^-$ is fully motile at all agar concentrations revealing that *cheA1* is not required for surface motility (**Figure 4B**). Similar phenotypes were observed with the Pto1108

Deleted: We quantified surface motility in wild type PtoDC3000, PtoDC3000 Δ*fliC* (Clarke et al. 2013), PtoDC3000 Δ*pilA* (a T4 pili-deficient deletion mutant, (Roine et al. 1998)), and the PtoDC3000 *cheA2*$^-$ and PtoDC3000 *cheA1*$^-$ disruption mutants by inoculating KB plates with different agar concentrations (0.4-1.3%) that allow the observation of surface motility and measuring the maximum cross section of the spread of the bacteria on the plates.

chemotaxis disruption mutants except Pto1108 is unable to move effectively on high concentration agar (>1.2%) (**Figure S4A**). The same phenotypes were observed with second, independent disruption mutants of *cheA1* and *cheA2* in both the PtoDC3000 and Pto1108 background.

Surface but not swimming motility is temperature-dependent in *Pto*

Production of surfactants, flagella components and other products required for motility by *P. syringae* pv. *syringae* are thermo-regulated with expression reduced at temperatures greater than 25°C and completely repressed at 30°C (Hockett et al. 2013). We therefore tested both swimming and surface motility of all chemotaxis and motility mutant strains at both 21°C and 28°C to ascertain whether our previously observed motility phenotypes were affected by the temperature they were originally performed (28°C). All of the strains spread more slowly on swim plates at 21°C, which is closer to the optimal temperature for swimming motility (Cuppels 1988), than 28°C but had no effect on the phenotype of any mutant relative to wild type (**Figure S5**).

Conversely, the effects of knocking out chemotaxis and motility genes in Pto on surface motility was significantly temperature-dependent. PtoDC3000 Δ*pilA* was motile on both 0.5% and 0.9% agar at 21°C but not at 28°C (**Figure 5A, B**), suggesting a *pilA*-independent motility mechanism in Pto for motility on semi-solid surfaces that is repressed at higher temperatures. PtoDC3000 Δ*fliC* and PtoDC3000 *cheA2*$^{-}$ were only able to spread at 28°C but not 21°C (**Figure 5C,D**). Again *cheA1* was not essential for surface motility under any conditions (**Figure 5C,D**). Moreover, *cheA1* was not essential for surface motility in strain Pto1108 at any temperature tested (**Figures S4B**). Pto1108*cheA2*$^{-}$ was also motile on higher agar concentrations (0.9%) at 28°C but not 21°C (**Figure S4B**) suggesting temperature regulation of swarming motility in this strain as well.

Deleted: B, D

Deleted: A-

Deleted: A-

Both chemotaxis pathways are required for full *in planta* fitness of Pto

To test the importance of chemotaxis during plant-Pto interactions, tomato plants (*Solanum lycopersicum* cv. Heinz) were spray inoculated with either wild type or chemotaxis disruption mutant strains of Pto. Total *in planta* bacterial population sizes were quantified 4 days post inoculation. Both chemotaxis pathways are necessary for full *in planta* fitness of both PtoDC3000 and Pto1108 (**Figure 6A**), and *cheA2* is essential for full pathogenicity of Pto1108 in tomato (**Figure 6B**), though there was substantial variability within and among independent experiments potentially reflecting small differences in humidity or other environmental conditions. Additionally, both chemotaxis mutants of PtoDC3000 have reduced fitness on *A. thaliana* (another plant host of PtoDC3000, **Figure 6C**), suggesting that pathogen chemotaxis is an important factor in multiple plant-microbe interactions. This phenotype was confirmed with independent disruption mutants for all strain-plant combinations. The reduced growth is not due to general fitness defects as the chemotaxis disruption mutants grow as well as the wild type strain in liquid culture (**Figure 3, Figure S3A**). Neither *cheA1* nor *cheA2* was essential for pathogenicity when inoculated via infiltration directly into the apoplast of *A. thaliana* or tomato (**Figure S6**). We therefore conclude that the chemotaxis pathways are primarily functioning during the epiphytic phase of Pto plant infection. All plant infections were confirmed at least

Deleted: and quantified total *in planta* bacterial population sizes.

Deleted: y

twice with independent *cheA* disruption mutants, but ectopic expression of *cheA1* or *cheA2* was insufficient to consistently rescue plant pathogenicity.

Disruption of the *che2* pathway increases the fitness of *Pto* strain 1108 on the non-host pathogen *A. thaliana*

In contrast to the attenuated growth of the chemotaxis mutants on susceptible plants, Pto1108:*cheA2*- grew to significantly higher population densities than wild type Pto1108 on *A. thaliana*, a non-host plant for Pto1108 (**Figure 6D**). This result indicates that functional chemotactic systems contribute to the resistance phenotype in this non-host interaction.

Discussion

Mutations in chemosensory systems underscore recent clonal shifts in field populations of Pto

The worldwide field population of Pto has undergone a significant population shift with the PtoT1 lineage becoming the dominant clone over the past 60 years (Cai et al. 2011). Comparisons between the genomes of Pto1108, an early PtoT1 strain, and several more recent PtoT1 strains revealed that several putative chemotaxis-associated genes are under selection in the now dominant PtoT1 lineage. This pattern suggests that changes in chemotactic systems may be adaptations underpinning the Pto population shift. Before testing this hypothesis, it was necessary to first test the broader hypothesis that chemotaxis pathways are functional in - and important for - Pto during its lifecycle.

The *che2* pathway, but not the *che1* pathway, is required for multiple Pto motility mechanisms

We identified multiple chemotaxis clusters in the Pto genome (**Figure 1**) and tentatively proposed that the *che2* cluster encodes the canonical flagella-controlling chemotaxis pathway based on sequence and syntenic similarity to chemotaxis pathways in other gram-negative bacteria. All tested *cheA2* disruption and deletion mutants were phenotypically identical to the flagella-minus *fliC* mutant in swim plates, split capillary assays, and surface motility assays (**Figure 2, Figure 4**). We therefore conclude that the *che2* pathway is the canonical chemotaxis pathway in Pto controlling flagellar motility.

The function of the *che1* pathway in Pto remains a mystery. We had hypothesized that the *che1* pathway was controlling pili-dependent twitching motility because of its sequence and syntenic similarity to the pili-controlling chemotaxis cluster in *P. aeruginosa* (Whitchurch et al. 2004) and its genomic position next to pili biosynthesis genes (**Figure 1**). However, this hypothesis was not supported by our data because the *cheA1* mutants behaved identically to the wild type Pto strains in surface motility (**Figure 4**). The PtoDC3000 Δ*pilA* strain did, as expected, exhibit aberrant surface motility behavior.

Pto has multiple temperature-dependent surface motility mechanisms based on the divergent phenotypes observed at 28°C compared to 21°C. Unlike *P. syringae* pv. *syringae* (Hockett et al. 2013), surface motility of wild type Pto was not markedly affected at 28°C compared to 21°C. However, putative swarming motility was likely downregulated at 28°C but was compensated for by twitching motility in Pto. Specifically, we found that Pto has an additional *fliC*- and *cheA2*-dependent surface motility mechanism as previously shown (Nogales et al. 2015), which is

Deleted: , though again we observed significant experiment-to-experiment variability.

Deleted: Delivery of avirulent effector proteins, such as AvrRpt2, is a major component of the non-host resistance of *A. thaliana* against Pto strains (Almeida et al. 2009; Sohn et al. 2012). We therefore hypothesized that knocking out the *che2* pathway attenuates the delivery of effector proteins into plant cells through an unknown mechanism. However, neither *cheA1* nor *cheA2* was required for PtoDC3000 to trigger an *avrRpt2*-dependent hypersensitive response in *A. thaliana* (**Figure 6E**).

active only at higher temperatures. *pilA* was essential for surface motility at 28°C and *fliC* and *cheA2* were essential for surface motility at 21°C (**Figure 5**) revealing that Pto has at least two genetically distinct mechanisms for surface motility, both of which are *cheA1*-independent. These results suggest that swarming motility is favored at lower temperatures and twitching motility favored at higher temperatures for Pto. The nature of these distinct mechanisms and how *Pto* switches from a *fliC/cheA2*-dependent to a *pilA*-dependent motility mechanism as temperatures increase remains to be elucidated.

Pto requires functional chemotaxis for optimal plant pathogenicity

P. syringae strains, including Pto, can live in myriad environments but are most intensively studied for their role as the causative agents of plant disease. The identified chemotaxis pathways are potentially used in numerous phases of the Pto lifecycle. In this work we establish that fitness of Pto on host plants is potentially dependent on both the *che2* and *che1* pathways (**Figure 6**) though high experiment-to-experiment variability remains an issue. The function of the *che1* pathway remains unknown, precluding speculation about the mechanism by which mutations in *cheA1* reduce the fitness of Pto in plants. The primary role of the *che2* pathway appears to be regulating rotational bias of the flagellar motor and we presume that the primary cause of the fitness defect associated with mutations in *cheA2* in Pto is a result of the loss of flagella-dependent motility. However, in previous work we established that the PtoDC3000Δ*fliC* strain is not required for optimal pathogenicity of plants following spray inoculation (Clarke et al. 2013). It is therefore challenging to interpret the finding that *cheA2* mutants are less fit on plant hosts. We propose that either 1) the *che2* pathway is required by Pto for functions other than flagellar motor control during plant infections, or 2) the wild type-level pathogenicity of the PtoDC3000Δ*fliC* strain on tomato is the result of a counterbalance between a decrease in pathogenicity due to loss of flagella function and an increase in pathogenicity due to loss of several flagellin-derived elicitors of plant immunity (Clarke et al. 2013).

This conclusion warrants caution because ectopic expression of *cheA* did not rescue the pathogenicity of the *cheA* disruption mutants and experiment-to-experiment variability. We hypothesize that complementation is not successful in this case to rescue the pathogenicity because of potential polar effects on genes in the *che* clusters downstream of *cheA*. This hypothesis is supported by the observation that ectopic expression of *cheA2* in the PtoDC3000 *cheA2*$^-$ strain only partially restored swimming motility (**Figure 2A**). Though ectopic expression of *cheA2* fully rescued swimming motility in the PtoDC3000 Δ*cheA2* strain, we were unable to use the deletion mutants in the plant pathogenicity assays because of a general growth defect in these strains (**Figure S3B**).

Regarding, the variability of the severity of attenuation of plant pathogenicity of *cheA1* and *cheA2* mutants, we propose that the effect is dependent on specific environmental conditions (such as humidity, daytime, and temperature (Hirano & Upper 2000; Wilson et al. 1999)). Our finding that Pto alters its predominant mechanism of surface motility based on temperature **(Figure 5)** supports the proposition of environmental conditions playing a crucial role in determining plant pathogenicity. The optimal growth conditions for Pto to use chemotaxis to maximize plant pathogenicity remain to be determined. It is important to note that alterations in

in planta fitness of the disruption mutants was confirmed using second independent disruption mutants. Additionally, differences were only observed in one direction; no experiments resulted in the opposite phenotype shown in Figure 6. Finally, both *cheA1* and *cheA2* mutants were only essential for pathogenicity following spray-inoculation, not infiltration-inoculation. We therefore propose that Pto is primarily using its chemosensory system during the epiphytic phase of plant infection that is bypassed during infiltration-inoculation. Future experiments to distinguish epiphytic vs. endophytic growth of Pto and the chemotaxis mutants will help clarify this possibility.

Functional chemotaxis pathways are detrimental to Pto1108 in a non-host interaction

Surprisingly, Pto1108 *cheA2*$^{-}$ was a more successful pathogen than wild type Pto1108 on the non-host plant *Arabidopsis* (**Figure 6D**), though again we observed significant experiment-to-experiment variability. However, it is worth noting that Pto1108 *cheA2*$^{-}$ grew better or the same as wild type Pto1108 in all experiments and never worse than wild type. We hypothesize that this increase in pathogenicity is a result of Pto1108 *cheA2*$^{-}$ strain triggering a weaker immune response in *A. thaliana* than wild type Pto1108. Specifically, we propose that Pto1108 *cheA2*$^{-}$ triggers fewer *A. thaliana* defenses, because it has an extended epiphytic phase avoiding detection by the plant immune system. In this model, loss of chemotactic control of the flagellar motor results in the strain being unable to locate stomata or other openings into the apoplast. This inability to switch from an epiphytic to an endophytic lifestyle is harmful for strains on host plants because they are equipped to avoid and suppress the plant immune system while invading the nutrient rich apoplast and escaping UV and desiccation stress on the leaf surface (Wilson et al. 1999) and therefore benefit from becoming endophytes. Alternatively, during infection of non-host plants, the microbe benefits from remaining epiphytic, because it is ill-equipped to suppress the strong plant immune responses activated during endophytic invasion. Experimental evidence for both the attenuated elicitation of plant immune responses and extended epiphytic lifestyle of *cheA2* mutants will greatly strengthen confidence in this model.

Conclusions

These results demonstrate the importance of the chemotactic systems of Pto for bacterial motility and pathogenicity in plants. We identified and characterized the *che2* cluster as the chemotaxis cluster that regulates flagellar-dependent swimming motility and swarming surface motility. Surface motility of Pto is likely thermo-regulated with swarming motility favored at low temperatures (21^{o}C) and twitching motility favored at higher temperatures (28^{o}C). The *che2* cluster is also essential for optimized pathogenicity of Pto1108 and PtoDC3000 on plant hosts, potentially during the epiphytic phase of plant invasion. The *che1* cluster also plays a potential role in PtoDC3000 pathogenicity of tomato though the role of *che1* in motility remains unresolved.

Building upon this foundation, it will be possible to exploit the natural variation in chemotaxis genes to discover if chemosensory systems contribute to the host range and adaptation of Pto strains and other bacterial plant pathogens. Specifically, future work can address the hypothesis

Comment [JHC3]:

Deleted: The non-host resistance of *A. thaliana* against PtoT1 (a strain with over 99.999% DNA identity to Pto1108 (Cai et al. 2011)) is largely dependent on recognition of avirulent effector proteins (Almeida et al. 2009; Sohn et al. 2012). However, neither *cheA1* nor *cheA2* was required for delivery of the effector protein AvrRpt2 into plant cells (**Figure 6E**).

Deleted: We alternatively

Deleted: likely specifically

519 that the seven identified non-synonymous SNPs in MCPs contribute to improved fitness of the
520 recent PtoT1 strains in tomato field populations.

521 **Acknowledgements**

522 We sincerely thank Ben Webb (VT) for technical guidance, Joshua Clarke for assistance with
523 plotting in Matlab, and Birgit Scharf (VT) for technical guidance and critical review of the
524 manuscript.

525 **References**

526 Adler J. 1973. A Method for Measuring Chemotaxis and Use of the Method to Determine Optimum
527 Conditions for Chemotaxis by *Escherichia coli*. *Microbiology* 74:77-91. doi:10.1099/00221287-
528 74-1-77
529 Almeida NF, Yan S, Lindeberg M, Studholme DJ, Schneider DJ, Condon B, Liu H, Viana CJ, Warren A,
530 Evans C, Kemen E, MacLean D, Angot A, Martin GB, Jones JD, Collmer A, Setubal JC, and Vinatzer
531 BA. 2009. A Draft Genome Sequence of *Pseudomonas syringae* pv. *tomato* T1 Reveals a Type III
532 Effector Repertoire Significantly Divergent from That of *Pseudomonas syringae* pv. *tomato*
533 DC3000. *Molecular Plant-Microbe Interactions* 22:52-62. 10.1094/MPMI-22-1-0052
534 Aravind L, and Ponting CP. 1999. The cytoplasmic helical linker domain of receptor histidine kinase and
535 methyl-accepting proteins is common to many prokaryotic signalling proteins. *FEMS*
536 *Microbiology Letters* 176:111-116. 10.1016/s0378-1097(99)00197-4
537 Bahar O, Goffer T, and Burdman S. 2009. Type IV Pili Are Required for Virulence, Twitching Motility, and
538 Biofilm Formation of Acidovorax avenae subsp. citrulli. *Molecular Plant-Microbe Interactions*
539 22:909-920. 10.1094/mpmi-22-8-0909
540 Bao Z, Cartinhour S, and Swingle B. 2012. Substrate and Target Sequence Length Influence RecTE(Psy)
541 Recombineering Efficiency in Pseudomonas syringae. *PLoS One* 7:e50617.
542 10.1371/journal.pone.0050617
543 Bao Z, Stodghill PV, Myers CR, Lam H, Wei H-L, Chakravarthy S, Kvitko BH, Collmer A, Cartinhour SW,
544 Schweitzer P, and Swingle B. 2014. Genomic Plasticity Enables Phenotypic Variation of
545 *Pseudomonas syringae* pv. *tomato* DC3000. *PLoS ONE* 9:e86628. 10.1371/journal.pone.0086628
546 Berg HC, and Brown DA. 1972. Chemotaxis in *Escherichia coli* analysed by Three-dimensional Tracking.
547 *Nature* 239:500-504.
548 Blattner FR, Plunkett G, Bloch CA, Perna NT, Burland V, Riley M, Collado-Vides J, Glasner JD, Rode CK,
549 Mayhew GF, Gregor J, Davis NW, Kirkpatrick HA, Goeden MA, Rose DJ, Mau B, and Shao Y. 1997.
550 The Complete Genome Sequence of *Escherichia coli* K-12. *Science* 277:1453-1462.
551 10.1126/science.277.5331.1453
552 Buell CR, Joardar V, Lindeberg M, Selengut J, Paulsen IT, Gwinn ML, Dodson RJ, Deboy RT, Durkin AS,
553 Kolonay JF, Madupu R, Daugherty S, Brinkac L, Beanan MJ, Haft DH, Nelson WC, Davidsen T,
554 Zafar N, Zhou L, Liu J, Yuan Q, Khouri H, Fedorova N, Tran B, Russell D, Berry K, Utterback T, Van
555 Aken SE, Feldblyum TV, D'Ascenzo M, Deng W-L, Ramos AR, Alfano JR, Cartinhour S, Chatterjee
556 AK, Delaney TP, Lazarowitz SG, Martin GB, Schneider DJ, Tang X, Bender CL, White O, Fraser CM,
557 and Collmer A. 2003. The complete genome sequence of the Arabidopsis and tomato pathogen
558 *Pseudomonas syringae* pv. *tomato* DC3000. *Proceedings of the National Academy of Sciences*
559 100:10181-10186. 10.1073/pnas.1731982100
560 Cai R, Lewis J, Yan S, Liu H, Clarke CR, Campanile F, Almeida NF, Studholme DJ, Lindeberg M, Schneider
561 D, Zaccardelli M, Setubal JC, Morales-Lizcano NP, Bernal A, Coaker G, Baker C, Bender CL, Leman
562 S, and Vinatzer BA. 2011. The Plant Pathogen *Pseudomonas syringae* pv. *tomato* Is Genetically

Monomorphic and under Strong Selection to Evade Tomato Immunity. *PLoS Pathog* 7:e1002130. 10.1371/journal.ppat.1002130

Clarke CR, Cai R, Studholme DJ, Guttman DS, and Vinatzer BA. 2010. *Pseudomonas syringae* Strains Naturally Lacking the Classical *P. syringae hrp/hrc* Locus Are Common Leaf Colonizers Equipped with an Atypical Type III Secretion System. *Molecular Plant-Microbe Interactions* 23:198-210. 10.1094/MPMI-23-2-0198

Clarke CR, Chinchilla D, Hind SR, Taguchi F, Miki R, Ichinose Y, Martin GB, Leman S, Felix G, and Vinatzer BA. 2013. Allelic variation in two distinct *Pseudomonas syringae* flagellin epitopes modulates the strength of plant immune responses but not bacterial motility. *New Phytologist* 200:847-860. 10.1111/nph.12408

Clarke CR, Hayes BW, Runde BJ, Wicker E, and Vinatzer BA. 2014. Eggplant and related species are promising genetic resources to dissect the plant immune response to *Pseudomonas syringae* and *Xanthomonas euvesicatoria* and to identify new resistance determinants. *Molecular Plant Pathology* 15:814-822. 10.1111/mpp.12140

Cuppels DA. 1988. Chemotaxis by *Pseudomonas syringae* pv. *tomato*. *Applied and Environmental Microbiology* 54:629-632.

Darzins A. 1994. Characterization of a Pseudomonas aeruginosa gene cluster involved in pilus biosynthesis and twitching motility: sequence similarity to the chemotaxis proteins of enterics and the gliding bacterium Myxococcus xanthus. *Molecular Microbiology* 11:137-153. 10.1111/j.1365-2958.1994.tb00296.x

De La Fuente L, Burr TJ, and Hoch HC. 2008. Autoaggregation of *Xylella fastidiosa* Cells Is Influenced by Type I and Type IV Pili. *Applied and Environmental Microbiology* 74:5579-5582. 10.1128/aem.00995-08

Ferrández A, Hawkins AC, Summerfield DT, and Harwood CS. 2002. Cluster II *che* Genes from *Pseudomonas aeruginosa* Are Required for an Optimal Chemotactic Response. *Journal of Bacteriology* 184:4374-4383. 10.1128/jb.184.16.4374-4383.2002

Hawes MC, and Smith YL. 1989. Requirement for chemotaxis in pathogenicity of Agrobacterium tumefaciens on roots of soil-grown pea plants. *Journal of Bacteriology* 171:5668-5671.

Hickman JW, Tifrea DF, and Harwood CS. 2005. A chemosensory system that regulates biofilm formation through modulation of cyclic diguanylate levels. *Proceedings of the National Academy of Sciences of the United States of America* 102:14422-14427. 10.1073/pnas.0507170102

Hirano SS, and Upper CD. 2000. Bacteria in the Leaf Ecosystem with Emphasis on *Pseudomonas syringae*—a Pathogen, Ice Nucleus, and Epiphyte. *Microbiology and Molecular Biology Reviews* 64:624-653. 10.1128/mmbr.64.3.624-653.2000

Hockett KL, Burch AY, and Lindow SE. 2013. Thermo-Regulation of Genes Mediating Motility and Plant Interactions in *Pseudomonas syringae*. *PLoS ONE* 8:e59850. 10.1371/journal.pone.0059850

Huynh TV, Dahlbeck, D., Staskawicz, B. J. . 1989. Bacterial blight of soybean: Regulation of a pathogen gene determining host cultivar specificity. *Science* 245:1374-1375.

Joardar V, Lindeberg M, Jackson RW, Selengut J, Dodson R, Brinkac LM, Daugherty SC, DeBoy R, Durkin AS, Giglio MG, Madupu R, Nelson WC, Rosovitz MJ, Sullivan S, Crabtree J, Creasy T, Davidsen T, Haft DH, Zafar N, Zhou L, Halpin R, Holley T, Khouri H, Feldblyum T, White O, Fraser CM, Chatterjee AK, Cartinhour S, Schneider DJ, Mansfield J, Collmer A, and Buell CR. 2005. Whole-Genome Sequence Analysis of *Pseudomonas syringae* pv. *phaseolicola* 1448A Reveals Divergence among Pathovars in Genes Involved in Virulence and Transposition. *Journal of Bacteriology* 187:6488-6498. 10.1128/jb.187.18.6488-6498.2005

Kamoun S, and Kado CI. 1990. Phenotypic Switching Affecting Chemotaxis, Xanthan Production, and Virulence in Xanthomonas campestris. *Appl Environ Microbiol* 56:3855-3860.

Kato J, Kim H-E, Takiguchi N, Kuroda A, and Ohtake H. 2008. *Pseudomonas aeruginosa* as a model microorganism for investigation of chemotactic behaviors in ecosystem. *Journal of Bioscience and Bioengineering* 106:1-7. http://dx.doi.org/10.1263/jbb.106.1

King EO, Ward MK, and Raney DE. Two simple media for the demonstration of pyocyanin and fluorescin. *Translational Research* 44:301-307. 10.5555/uri:pii:002221435490222X

Kirby JR. 2009. Chemotaxis-Like Regulatory Systems: Unique Roles in Diverse Bacteria. *Annual Review of Microbiology* 63:45-59. doi:10.1146/annurev.micro.091208.073221

Kunst F, Ogasawara N, Moszer I, Albertini AM, Alloni G, Azevedo V, Bertero MG, Bessieres P, Bolotin A, Borchert S, Borriss R, Boursier L, Brans A, Braun M, Brignell SC, Bron S, Brouillet S, Bruschi CV, Caldwell B, Capuano V, Carter NM, Choi SK, Codani JJ, Connerton IF, Cummings NJ, Daniel RA, Denizot F, Devine KM, Dusterhoft A, Ehrlich SD, Emmerson PT, Entian KD, Errington J, Fabret C, Ferrari E, Foulger D, Fritz C, Fujita M, Fujita Y, Fuma S, Galizzi A, Galleron N, Ghim SY, Glaser P, Goffeau A, Golightly EJ, Grandi G, Guiseppi G, Guy BJ, Haga K, Haiech J, Harwood CR, Henaut A, Hilbert H, Holsappel S, Hosono S, Hullo MF, Itaya M, Jones L, Joris B, Karamata D, Kasahara Y, Klaerr-Blanchard M, Klein C, Kobayashi Y, Koetter P, Koningstein G, Krogh S, Kumano M, Kurita K, Lapidus A, Lardinois S, Lauber J, Lazarevic V, Lee SM, Levine A, Liu H, Masuda S, Mauel C, Medigue C, Medina N, Mellado RP, Mizuno M, Moestl D, Nakai S, Noback M, Noone D, O'Reilly M, Ogawa K, Ogiwara A, Oudega B, Park SH, Parro V, Pohl TM, Portetelle D, Porwollik S, Prescott AM, Presecan E, Pujic P, Purnelle B, Rapoport G, Rey M, Reynolds S, Rieger M, Rivolta C, Rocha E, Roche B, Rose M, Sadaie Y, Sato T, Scanlan E, Schleich S, Schroeter R, Scoffone F, Sekiguchi J, Sekowska A, Seror SJ, Serror P, Shin BS, Soldo B, Sorokin A, Tacconi E, Takagi T, Takahashi H, Takemaru K, Takeuchi M, Tamakoshi A, Tanaka T, Terpstra P, Tognoni A, Tosato V, Uchiyama S, Vandenbol M, Vannier F, Vassarotti A, Viari A, Wambutt R, Wedler E, Wedler H, Weitzenegger T, Winters P, Wipat A, Yamamoto H, Yamane K, Yasumoto K, Yata K, Yoshida K, Yoshikawa HF, Zumstein E, Yoshikawa H, and Danchin A. 1997. The complete genome sequence of the Gram-positive bacterium *Bacillus subtilis*. *Nature* 390:249-256.

Li Y, Hao G, Galvani CD, Meng Y, Fuente LDL, Hoch HC, and Burr TJ. 2007. Type I and type IV pili of *Xylella fastidiosa* affect twitching motility, biofilm formation and cell–cell aggregation. *Microbiology* 153:719-726. doi:10.1099/mic.0.2006/002311-0

Matas IM, Lambertsen L, Rodríguez-Moreno L, and Ramos C. 2012. Identification of novel virulence genes and metabolic pathways required for full fitness of Pseudomonas savastanoi pv. savastanoi in olive (Olea europaea) knots. *New Phytologist* 196:1182-1196. 10.1111/j.1469-8137.2012.04357.x

Melotto M, Underwood W, Koczan J, Nomura K, and He SY. 2006. Plant Stomata Function in Innate Immunity against Bacterial Invasion. *Cell* 126:969-980.

Miller LD, Yost CK, Hynes MF, and Alexandre G. 2007. The major chemotaxis gene cluster of Rhizobium leguminosarum bv. viciae is essential for competitive nodulation. *Molecular Microbiology* 63:348-362. 10.1111/j.1365-2958.2006.05515.x

Moreira LM, Facincani AP, Ferreira CB, Ferreira RM, Ferro MIT, Gozzo FC, de Oliveira JCF, Ferro JA, and Soares MR. 2015. Chemotactic signal transduction and phosphate metabolism as adaptive strategies during citrus canker induction by *Xanthomonas citri*. *Functional & Integrative Genomics* 15:197-210. 10.1007/s10142-014-0414-z

Morris PF, and Ward EWB. 1992. Chemoattraction of zoospores of the soybean pathogen, Phytophthora sojae, by isoflavones. *Physiological and Molecular Plant Pathology* 40:17-22. 10.1016/0885-5765(92)90067-6

Nguyen LC, Taguchi F, Tran QM, Naito K, Yamamoto M, Ohnishi-Kameyama M, Ono H, Yoshida M, Chiku K, Ishii T, Inagaki Y, Toyoda K, Shiraishi T, and Ichinose Y. 2012. Type IV pilin is glycosylated in

Pseudomonas syringae pv. tabaci 6605 and is required for surface motility and virulence. *Molecular Plant Pathology* 13:764-774. 10.1111/j.1364-3703.2012.00789.x

Nogales J, Vargas P, Farias GA, Olmedilla A, Sanjuán J, and Gallegos M-T. 2015. FleQ Coordinates Flagellum-Dependent and -Independent Motilities in *Pseudomonas syringae* pv. *tomato* DC3000. *Applied and Environmental Microbiology* 81:7533-7545. 10.1128/aem.01798-15

Oku S, Komatsu A, Tajima T, Nakashimada Y, and Kato J. 2012. Identification of Chemotaxis Sensory Proteins for Amino Acids in *Pseudomonas fluorescens* Pf0-1 and Their Involvement in Chemotaxis to Tomato Root Exudate and Root Colonization. *Microbes and Environments* 27:462-469. 10.1264/jsme2.ME12005

Parkinson JS, Hazelbauer GL, and Falke JJ. 2015. Signaling and sensory adaptation in *Escherichia coli* chemoreceptors: 2015 update. *Trends in Microbiology* 23:257-266. http://dx.doi.org/10.1016/j.tim.2015.03.003

Parkinson JS, and Houts SE. 1982. Isolation and behavior of Escherichia coli deletion mutants lacking chemotaxis functions. *J Bacteriol* 151:106-113.

Porter SL, Wadhams GH, and Armitage JP. 2011. Signal processing in complex chemotaxis pathways. *Nat Rev Micro* 9:153-165.

Riepl H, Maurer T, Kalbitzer HR, Meier VM, Haslbeck M, Schmitt R, and Scharf B. 2008. Interaction of CheY2 and CheY2-P with the cognate CheA kinase in the chemosensory-signalling chain of Sinorhizobium meliloti. *Molecular Microbiology* 69:1373-1384. 10.1111/j.1365-2958.2008.06342.x

Roine E, Raineri DM, Romantschuk M, Wilson M, and Nunn DN. 1998. Characterization of Type IV Pilus Genes in *Pseudomonas syringae* pv. *tomato* DC3000. *Molecular Plant-Microbe Interactions* 11:1048-1056. 10.1094/MPMI.1998.11.11.1048

Scharf BE, Hynes MF, and Alexandre GM. 2016. Chemotaxis signaling systems in model beneficial plant–bacteria associations. *Plant Molecular Biology* 90:549-559. 10.1007/s11103-016-0432-4

Schmitt R. 2002. Sinorhizobial chemotaxis: a departure from the enterobacterial paradigm. *Microbiology* 148:627-631.

Shah DSH, Porter SL, Martin AC, Hamblin PA, and Armitage JP. 2000. Fine tuning bacterial chemotaxis: analysis of Rhodobacter sphaeroides behaviour under aerobic and anaerobic conditions by mutation of the major chemotaxis operons and cheY genes. *EMBO J* 19:4601-4613.

Sohn KH, Saucet SB, Clarke CR, Vinatzer BA, O'Brien HE, Guttman DS, and Jones JDG. 2012. HopAS1 recognition significantly contributes to *Arabidopsis* nonhost resistance to *Pseudomonas syringae* pathogens. *New Phytologist* 193:58-66. 10.1111/j.1469-8137.2011.03950.x

Sourjik V, and Schmitt R. 1996. Different roles of CheY1 and CheY2 in chemotaxis of Rhizobium meliloti. *Molecular Microbiology* 22:427-436.

Stock A, Koshland DE, and Stock J. 1985. Homologies between the *Salmonella typhimurium* CheY protein and proteins involved in the regulation of chemotaxis, membrane protein synthesis, and sporulation. *Proceedings of the National Academy of Sciences* 82:7989-7993.

Stover CK, Pham XQ, Erwin AL, Mizoguchi SD, Warrener P, Hickey MJ, Brinkman FSL, Hufnagle WO, Kowalik DJ, Lagrou M, Garber RL, Goltry L, Tolentino E, Westbrock-Wadman S, Yuan Y, Brody LL, Coulter SN, Folger KR, Kas A, Larbig K, Lim R, Smith K, Spencer D, Wong GKS, Wu Z, Paulsen IT, Reizer J, Saier MH, Hancock REW, Lory S, and Olson MV. 2000. Complete genome sequence of *Pseudomonas aeruginosa* PAO1, an opportunistic pathogen. *Nature* 406:959-964. http://www.nature.com/nature/journal/v406/n6799/suppinfo/406959a0_S1.html

Swingle B, Bao Z, Markel E, Chambers A, and Cartinhour S. 2010. Recombineering Using RecTE from Pseudomonas syringae. *Appl Environ Microbiol* 76:4960-4968.

703 Taguchi F, and Ichinose Y. 2011. Role of Type IV Pili in Virulence of Pseudomonas syringae pv. tabaci
704 6605: Correlation of Motility, Multidrug Resistance, and HR-Inducing Activity on a Nonhost
705 Plant. *Molecular Plant-Microbe Interactions* 24:1001-1011. 10.1094/mpmi-02-11-0026
706 Van de Broek A, Lambrecht M, and Vanderleyden J. 1998. Bacterial chemotactic motility is important for
707 the initiation of wheat root colonization by Azospirillum brasilense. *Microbiology* 144:2599-
708 2606. 10.1099/00221287-144-9-2599
709 Wadhams GH, and Armitage JP. 2004. Making sense of it all: bacterial chemotaxis. *Nat Rev Mol Cell Biol*
710 5:1024-1037.
711 Ward MJ, Bell AW, Hamblin PA, Packer HL, and Armitage JP. 1995. Identification of a chemotaxis operon
712 with two *cheY* genes in *Rhodobacter sphaeroides*. *Molecular Microbiology* 17:357-366.
713 10.1111/j.1365-2958.1995.mmi_17020357.x
714 Whitchurch CB, Leech AJ, Young MD, Kennedy D, Sargent JL, Bertrand JJ, Semmler ABT, Mellick AS,
715 Martin PR, Alm RA, Hobbs M, Beatson SA, Huang B, Nguyen L, Commolli JC, Engel JN, Darzins A,
716 and Mattick JS. 2004. Characterization of a complex chemosensory signal transduction system
717 which controls twitching motility in *Pseudomonas aeruginosa*. *Molecular Microbiology* 52:873-
718 893. 10.1111/j.1365-2958.2004.04026.x
719 Wilson M, Hirano SS, and Lindow SE. 1999. Location and Survival of Leaf-Associated Bacteria in Relation
720 to Pathogenicity and Potential for Growth within the Leaf. *Applied and Environmental*
721 *Microbiology* 65:1435-1443.
722 Yan S, Liu H, Mohr TJ, Jenrette J, Chiodini R, Zaccardelli M, Setubal JC, and Vinatzer BA. 2008. Role of
723 Recombination in the Evolution of the Model Plant Pathogen *Pseudomonas syringae* pv. *tomato*
724 DC3000, a Very Atypical Tomato Strain. *Applied and Environmental Microbiology* 74:3171-3181.
725 10.1128/aem.00180-08
726 Yao J, and Allen C. 2006. Chemotaxis Is Required for Virulence and Competitive Fitness of the Bacterial
727 Wilt Pathogen Ralstonia solanacearum. *J Bacteriol* 188:3697-3708. 10.1128/jb.188.10.3697-
728 3708.2006
729 Yu X, Lund SP, Scott RA, Greenwald JW, Records AH, Nettleton D, Lindow SE, Gross DC, and Beattie GA.
730 2013. Transcriptional responses of Pseudomonas syringae to growth in epiphytic versus
731 apoplastic leaf sites. *Proceedings of the National Academy of Sciences* 110:E425-E434.
732 10.1073/pnas.1221892110

733

734

735 **Table 1.** Strains used in this study.

Strain	Plasmid	Description	Source
Pto1108	6010:empty	wild type	This work
PtoDC3000	6010:empty	wild type	This work
Pto1108 *cheA1*$^{-}$	6010:empty	*cheA1* disruption mutant	This work
Pto1108 *cheA2*$^{-}$	6010:empty	*cheA2* disruption mutant	This work
Pto1108 *cheA1*$^{-}$(comp)	6010:*cheA1*	*cheA1* disruption mutant (complemented)	This work
Pto1108 *cheA2*$^{-}$(comp)	6010:*cheA2*	*cheA2* disruption mutant (complemented)	This work
PtoDC3000 *cheA1*$^{-}$	6010:empty	*cheA1* disruption mutant	This work
PtoDC3000 *cheA2*$^{-}$	6010:empty	*cheA2* disruption mutant	This work
PtoDC3000 *cheA1*$^{-}$(comp)	6010:*cheA1*	*cheA1* disruption mutant (complemented)	This work
PtoDC3000 *cheA2*$^{-}$(comp)	6010:*cheA2*	*cheA2* disruption mutant (complemented)	This work
PtoDC3000 Δ*cheA1*	6010:empty	*cheA1* deletion mutant	This work
PtoDC3000 Δ*cheA2*	6010:empty	*cheA2* deletion mutant	This work
PtoDC3000 Δ*cheA1* (comp)	6010:*cheA1*	*cheA1* deletion mutant (complemented)	This work
PtoDC3000 Δ*cheA2* (comp)	6010:*cheA2*	*cheA2* deletion mutant (complemented)	This work
PtoDC3000 Δ*fliC*	6010:empty	*fliC* deletion mutant	Clarke et al 2013
PtoDC3000 Δ*pilA*	6010:empty	*pilA* deletion mutant	Roine et al 1998

736

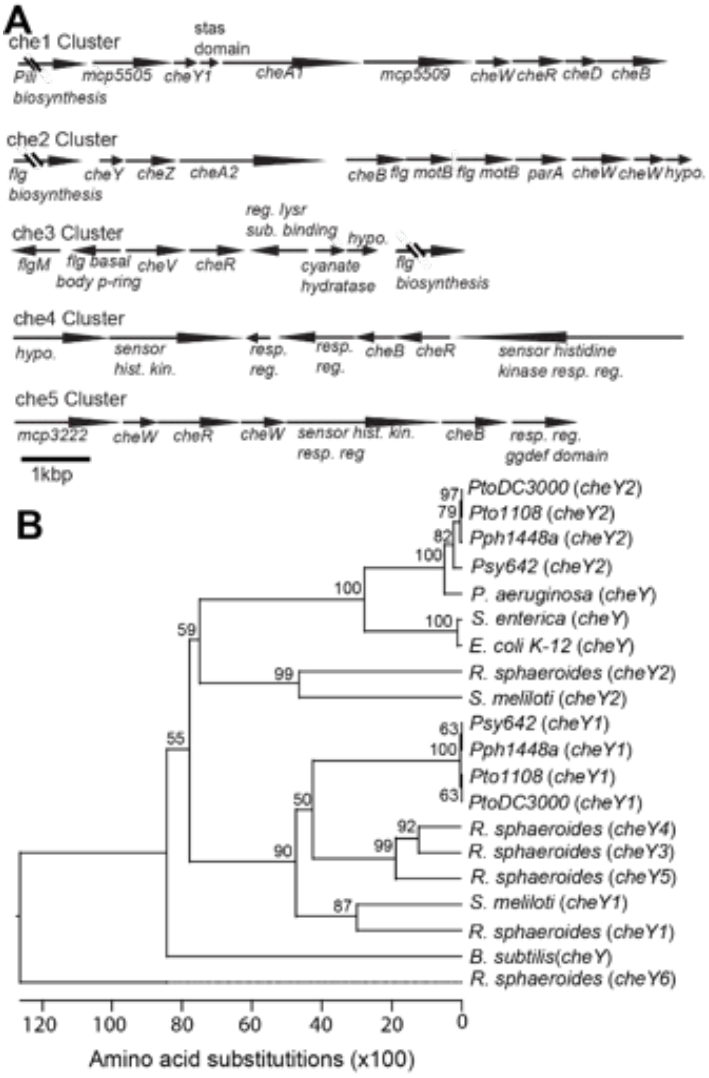

Figure 1. The genome of Pto1108 contains multiple chemotaxis gene clusters. **A.** The organization of the chemotaxis gene clusters in the genome of Pto1108. **B.** Neighbor-joining tree based on aligned CheY protein sequences from bacteria with previously characterized chemotaxis pathways and select other *P. syringae* strains. The full species and strain names are listed in the methods. Numbers at nodes represent bootstrap support based on 1000 trials.

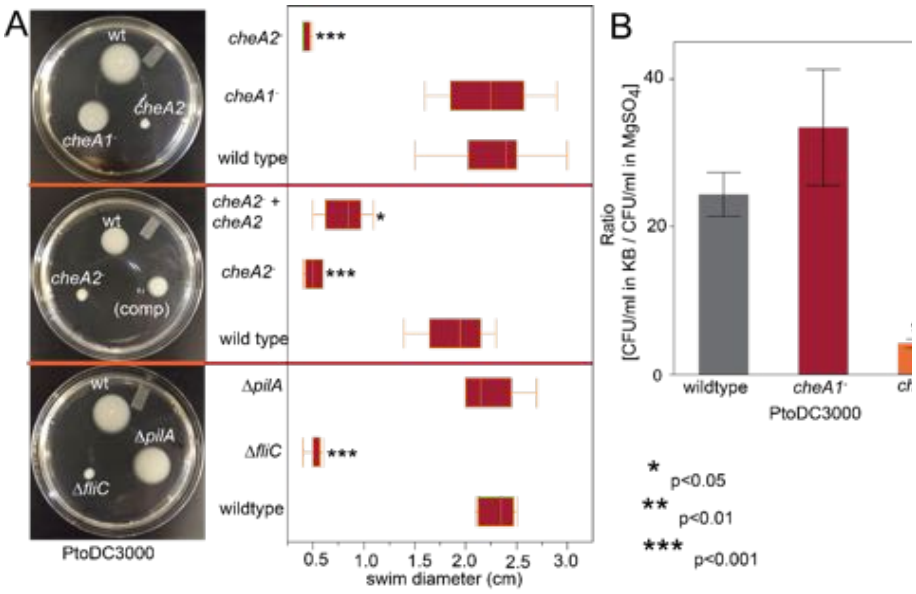

743

744 **Figure 2.** PtoDC3000:*cheA2*$^-$ strains are deficient in chemotactic swimming motility. **A.**
745 Example pictures and box plots of the colony diameter two days after inoculation of the
746 indicated strains on 0.28% agar KB swim plates. **B.** The ratio of colony forming units of the
747 indicated bacteria that entered a capillary tube of KB media over a capillary tube of 10 mM
748 $MgSO_4$ in the split capillary assay. Asterisks indicate statistical significance compared to wild
749 type in a Student's *t-test* at the indicated p-values. Data represent the average of 8 replicates and
750 error bars are the standard error. Essentially identical results were obtained in at least 3
751 independent experiments for all strains.

752

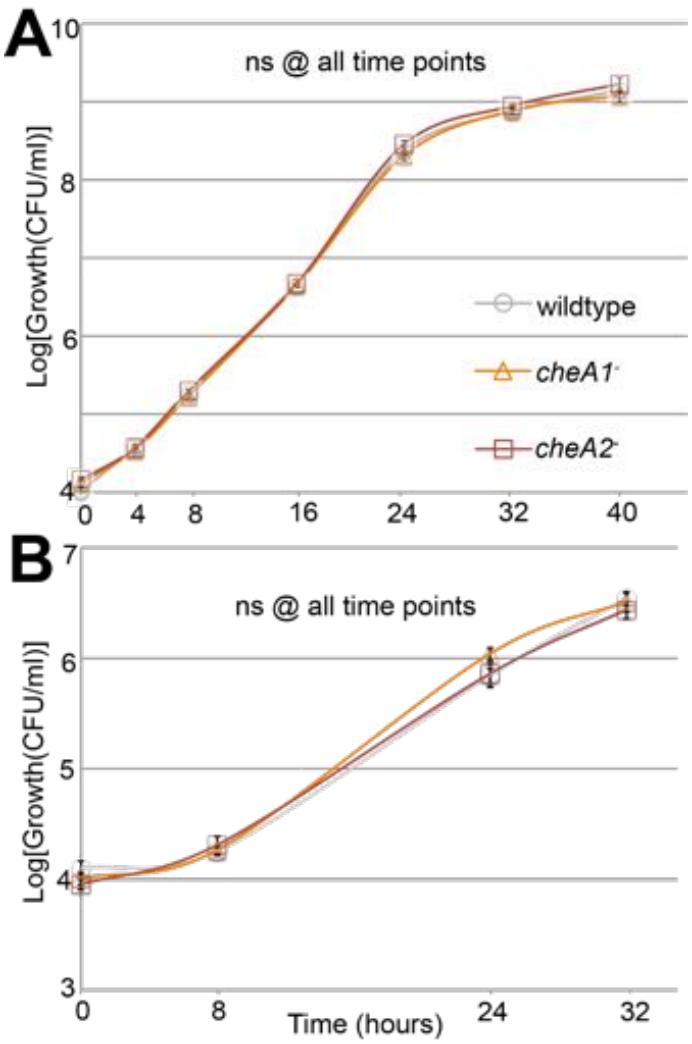

Figure 3. Neither *cheA1* nor *cheA2* is required for optimal growth of PtoDC3000 in liquid KB media. PtoDC3000, PtoDC3000 *cheA2*$^-$, and PtoDC3000 *cheA1*$^-$ were grown in liquid KB (**A**) and minimal media (**B**). ns = not significantly different from wild type in a Student's *t-test* at $p<0.05$. Data represent the average of 4 replicates and error bars are the standard error. Essentially identical results were obtained in 2 independent experiments.

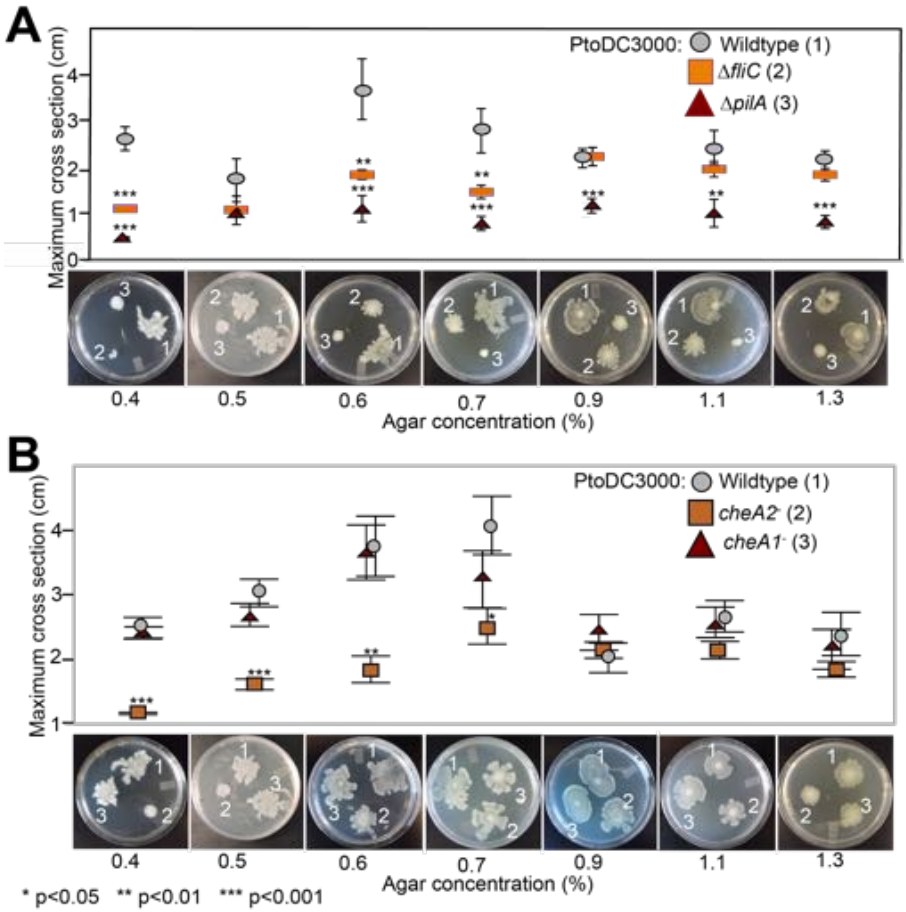

Figure 4. Neither *cheA1* nor *cheA2* is required for surface motility at 28°C. Data represent the average of 7 replicates and error bars are the standard error. * indicates significant differences in swim diameter for any strain between the two temperatures at the indicated p-values using a Student's *t-test*. Essentially identical results were obtained in at least 2 independent experiments for all strains at 0.4, 0.5, 0.6, 0.7, 0.9, 1.1 and 1.3% agar concentrations.

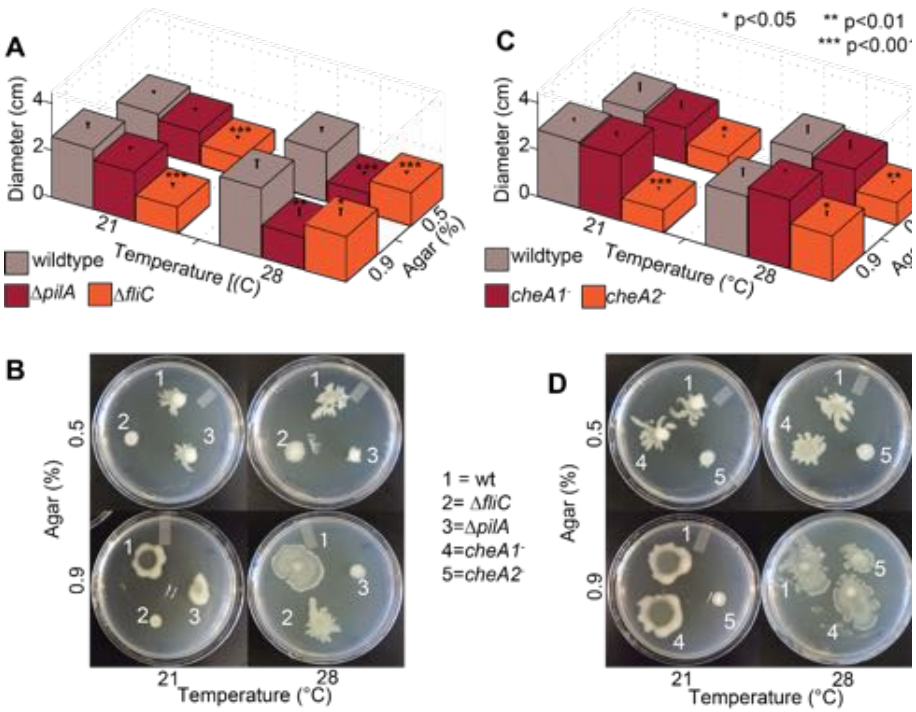

767

768 **Figure 5.** Both *pilA*-dependent and *cheA2/fliC*-dependent surface motility in PtoDC3000 are
769 thermo-regulated. Surface motility plate assays using 0.5% and 0.9% agar were performed with
770 the PtoDC3000 chemotaxis mutants (**A** and **C**) and the motility mutants (**B** and **D**) at both 28°C
771 and 21°C. Data represent the average of 8 replicates and error bars are the standard error. *
772 indicates significant differences in swarm diameter for any strain between the two temperatures
773 at the indicated p-values using a Student's *t-test*. Essentially identical results were obtained in at
774 least 3 independent experiments for all strains and all temperature/agar percentage combinations.

775

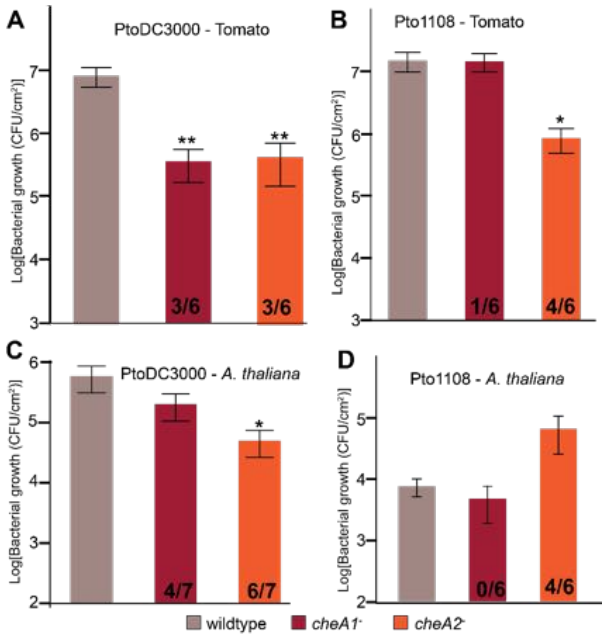

776

777 **Figure 6.** Disruptions in either the *che1* or *che2* pathway affect plant pathogenicity of Pto. **A-D.**
778 The population density of strain PtoDC3000 (**A** and **C**) or strain Pto1108 (**B** and **D**) 4 days
779 following spray inoculation of the indicated plants. Data represent the average of 6 replicates and
780 error bars are the standard error. Asterisks represent significant difference in a Student's t-test
781 between each mutant and the corresponding wild type strain (*, $p<0.05$, **, $p<0.01$). The
782 fraction of independent experiments resulting in at least a 5-fold difference in growth relative to
783 the wild type strain are shown at the bottom of the bar for each mutant strain.

784

Deleted: E. Neither *cheA1* nor *cheA2* is required for PtoDC3000 to elicit an *avrRpt2*-dependent HR in *A. thaliana*. Numbers underneath each representative picture indicate the number individual leaves that produced a strong HR 18 hours after infiltration with the indicated strains. Essentially identical results were obtained in two independent experiments.

Supplemental Information (separate files)

Tables S1-S2
Figures S1-S7
Author Contributions

Videos S1-S3

Raw data files